Journal of Hydrology (2008) 353, 76–92

available at www.sciencedirect.com

ScienceDirect

journal homepage: www.elsevier.com/locate/jhydrol

Modelling complex flood flow evolution in the middle Yellow River basin, China

Hongming He [a,b], Qian Yu [a,*], Jie Zhou [a], Yong Q. Tian [c], Robert F. Chen [c]

[a] *Department of GeoScience, University of Massachusetts-Amherst, Amherst, MA 01003, United States*
[b] *State Key Laboratory of Loess and Quaternary Geology, Institute of Earth Environment, Chinese Academy of Sciences, P.O. Box 17, Xian, 710075, China*
[c] *Department of Environmental, Earth and Ocean Sciences, University of Massachusetts, Boston, 100 Morrissey BLVD., Boston, MA 02125, United States*

Received 20 March 2007; received in revised form 17 January 2008; accepted 31 January 2008

KEYWORDS
Flood routing;
Backwater flow;
The middle Yellow River;
River morphology

Summary Flood routing processes in the middle Yellow River basin are complex since they consist of three types of flood: bidirectional, convergent and divergent flood flows between the main channel and its tributaries. We propose three computation schemes to simulate the complex flood routing: a simple scheme for a single main channel with no tributary or backwater, an improved schemes for convergent or divergent flow at the confluence, and an improved scheme for bidirectional flow. The schemes are examined by analyzing seven historical flood events and three scenarios of flood routing in the middle Yellow River basin. The model was calibrated and validated based on the simulation of three different types of flood. As compared with the observed hydrographs, the results show that the model is able to simulate flood routing processes efficiently for the study river (with Nash–Sutcliffe indices falling in the range 0.75–0.91). The model demonstrates that flood routing during historical flood events (1962–2003) in the middle Yellow River was altered under boundary condition changes. The shape of the hydrographs changed from high and thin to low and wide, which was accompanied by a delayed occurrence and extended duration of peak flow after the 1960s. Moreover, these trends were intensified after the early 1980s. Backwater resulted from divergent flows and bidirectional flood flows. An analysis of combined boundary conditions shows that flood wave volume has the strongest impact on flood duration, peak discharge and water level, the time of occurrence of peak discharge, and the magnitude of backwater. River bed slope has the second strongest impact on flood duration and the magnitude of backwater. Channel roughness has the second strongest impact on peak discharge and water level.
Published by Elsevier B.V.

* Corresponding author. Tel.: +1 413 5452095.
E-mail address: qyu@geo.umass.edu (Q. Yu).

0022-1694/$ - see front matter Published by Elsevier B.V.
doi:10.1016/j.jhydrol.2008.01.030

Introduction

Floods are one of the most common hazards in the middle Yellow River basin, China (Yu and Lin, 1996). Heavy flood events transport sediments from upstream to downstream and lead to changes of river channel morphology and flood routing processes (Speight, 1965; Beven et al., 1988; Carson and Griffiths, 1989; Wharton et al., 1989; Marston et al., 1995; Wyzga, 1997; Lee and Chang, 2005; Webb and Leake, 2006). One of the distinctive features of flood disasters in the middle Yellow River is that they mostly result water from backing up from downstream to upstream (Qian, 1992; Wang, 2004). Backwater from downstream dam and releases from tributaries extended the areas of floodplain. For decades, impacts of flood disasters of backwater have grown in spite of increasingly improved defence measures (Wang et al., 2005). From 1964 to 2003, there were 28 flood disasters of backwater from the middle Yellow River to the lower Weihe River (State Flood Control and Drought Relief Headquarters, 1992). These floods resulted in huge economic losses, increased inundated farmlands, and decreased crop productivity (He et al., 2006). An increased understanding of evolution of flood routing of backwater in the middle Yellow River would improve risk analysis and regional emergency response. Because the middle Yellow River is one of the major rivers in the world, the consequences of flood events in the middle Yellow River represent an international concern.

River channel morphology has significant impacts on flood routing. Quantification of the impacts involves estimating peak flow and characterizing hydraulic parameters. There were many previous efforts assessing the impacts of channel morphology on floods (Speight, 1965; Beven et al., 1988; Carson and Griffiths, 1989; Wharton et al., 1989; Wyzga, 1997; Lee and Chang, 2005; Webb and Leake, 2006). Speight (1965) studied the relationship between flow and channel characteristics and disclosed that migrating wide triangular channel cross-sections dominated by point-bars were more capable of carrying the most probable annual flood than fixed narrow rectangular sections dominated by levees with a sandy bed and silt—clay banks. Beven et al. (1988) examined the relationship of morphology to runoff routing and production in flood routing. They pointed out that morphology may be used as a clue to study hydrological responses. Based on the analysis of changes in vertical channel position and variations in flood flows, Wyzga (1997) revealed the importance of channel incision for increasing flood hazard to downstream reaches.

Many models for simulating flood routing were derived from the Saint-Venant equations (Daluz, 1983; Cunnane, 1988; Ramamurthy, 1990; Camacho and Lees, 1999; Carrivick, 2006) and other simplified wave models such as the kinematic wave, non-inertia wave, quasi-steady dynamic wave, and gravity wave approximations (Walters and Cheng, 1980; Begin, 1986). The model introduced by Chung et al. (1993) analyzed the response functions of flood wave movement in a semi-infinite channel and in a finite channel under general conditions. The model considered effects of downstream boundary conditions on diffusive flood routing and the magnitude of backwater. In their model, the inflow flood hydrograph was controlled by three parameters: the time to peak, the base time, and the peak discharge. Schurmans et al. (1995) used linearized Saint-Venant equations to analyze open-channel flow with backwater effects. The model emphasized the effects of backwater on frequency underestimation in the neighbourhood of the resonance in flood routing. Thorne and Furbish (1995) found that bank roughness essentially has backwater effects that resist surface flow downstream. Tsai (2005) theoretically investigated unsteady flow routing with downstream backwater effects in a mild-sloped river on the basis of linearized Saint-Venant equations and other routing models. The common issues reported in previous studies are that simplified kinematic wave and gravity wave models were unable to account for the downstream backwater effect and were not suitable for modelling the flood wave propagation in mild-sloped rivers.

These previous studies mostly dealt with the general form of flood routing. There is no appropriate solution to simulate the flood wave propagation with a downstream backwater effect of complex flood routing (such as bidirectional flow, convergent and divergent flows between the main channel and tributaries). At the same time, characteristics of different drainage systems affect flood differently, in terms of both duration and intensity (Goel et al., 2000). The characteristics include runoff volume, peak flow, and drainage channel morphology. Special attention needs to be paid to the investigation of the distinctive drainage characteristics of the middle Yellow River in the study of flood routing. On the other hand, the influence of tributary floods on the behaviour of water flows in the main channel has not been well studied in the middle Yellow River basin. There is a need to analyze the concurrent floods of multiple tributaries for improving our understanding of flood routing processes and the associated tributary drainage characteristics in a river basin.

The objective of this paper is to investigate the characteristics of flood wave propagation under different flood routing boundary conditions. By referencing to historic flood records in the study area, we analyze the impacts of flood propagation on regional environmental properties. This study examines the three computation schemes that we proposed for simulating the complex flood flows in the different boundary conditions and of varying inherent hydraulic features. These schemes are: a simple scheme for single main channel with no tributary and backwater, an improved scheme for convergent or divergent flow at the confluence, and an improved scheme for bidirectional flow. The simulation analysis improves our understanding of flood routing of backwater and complex flood flow evolution in the middle Yellow River.

Study area

The study area is located in the basin of the middle Yellow River (between Tongguan and Huaxian) at a latitude between 35°N and 38°N, and a longitude between 105°E and 112°E (Fig. 1). We focus on the main stem and its two tributaries, the Weihe River and the Luohe River. The Luohe River is the tributary of the Weihe River which flows into the middle Yellow River at Tongguan. The elevation of Tongguan rules the base level of the Weihe River, and influences the operation behaviours of the Sanmenxia Reservoir (construction in 1957—1960 and reconstruction in 1969—1978).

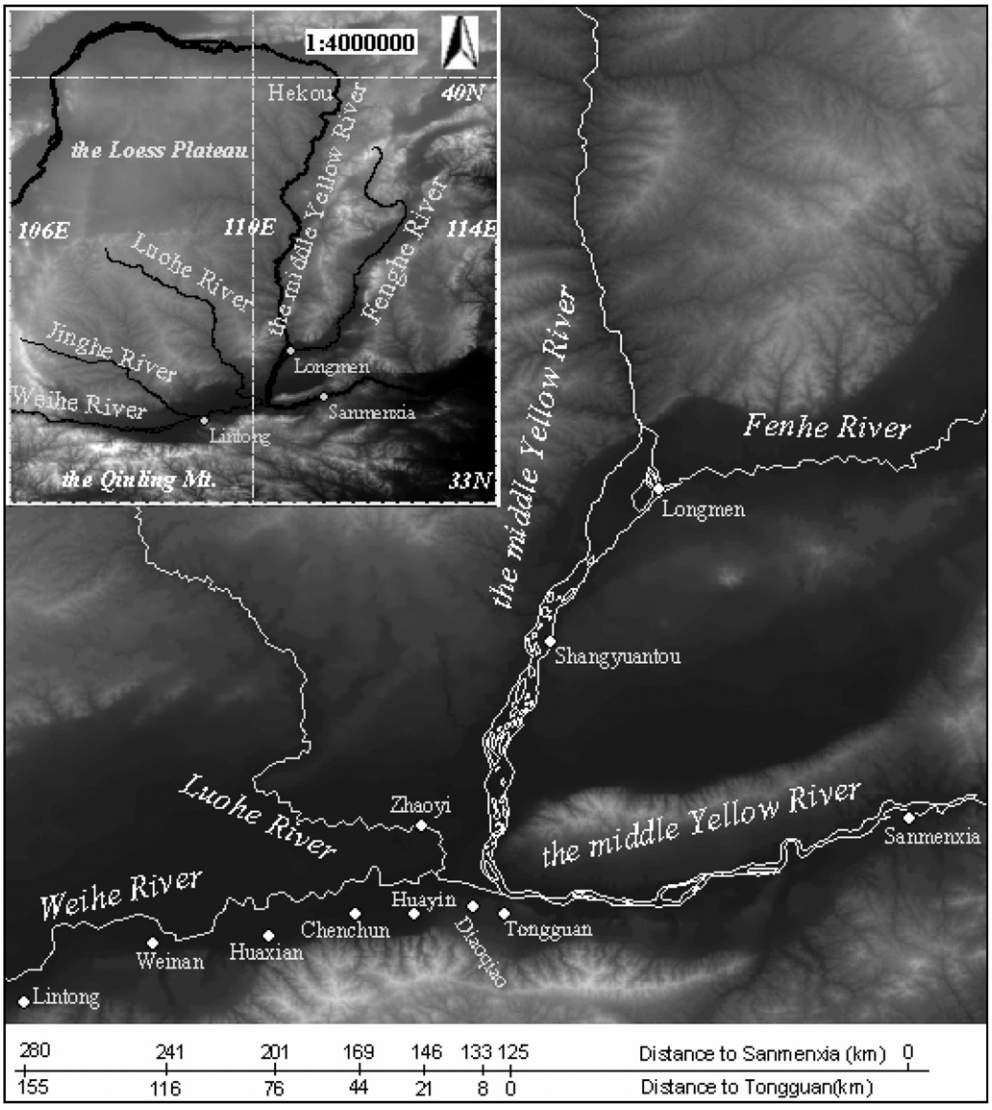

Figure 1 Location of study area in the middle Yellow River basin.

Annual precipitation in the study area ranges from 300 mm to 1000 mm per year. About 48% of the annual total (145—480 mm) falls in the summer season (from July to August) in the form of rainstorms (rainfall amounts are over 50 mm in 24 h). Floods occur frequently after rainstorms. They transport large amounts of sediments along the Weihe River and the middle Yellow River and deposit them in the lower Weihe River. The fluvial sediments gradually change river channel conditions, such as river bed elevation and roughness. Improper human activity, such as the construction of Sanmenxia Dam also contributed to the shrinkage of river channels in the study area. Consequently, backwater was caused in the middle Yellow River basin due to hydraulic condition changes.

The evolution of flood routing processes was examined at six cross-sections along the Weihe, Luohe River and middle Yellow Rivers. There are four water-gauge cross-sections from upstream to downstream in the Weihe River: Huaxian, Chenchun, Huayin and Tongguan. Two other cross-sections are at Zhaoyi in the Luohe River and at Shanyuantou in the middle Yellow River.

Material and methods

Data

In this study, input data to the simulation model include topographic, hydraulic and hydrometric datasets. Topographic data, such as river channel roughness, river bed slope, and distance between particular cross-sections, are extracted from the 30-m Digital Elevation Model (DEM, from IRSA, CAS). Hydraulic and hydrometric data such as flood flow radius, width, and cross-section area, and flood flow velocity, discharge and water level in each cross-section are obtained from gauge data compiled in the State Flood Control and Drought Relief Headquarters (State Flood Control and Drought Relief Headquarters, 1992). Gauge data of 11 flood events are collected in different time periods from 1954 to 2003, of which four flood events are used to calibrate the model, and four others are selected to examine the model efficiency through simulation results.

Computational schemes for complex flood flow evolution

Classification for steady and unsteady flow is necessary in describing the flows of interest. The simplest steady flow is uniform flow, in which no flow variable change with distance, and every flow variable is a constant with respect to distance and time (Keskin and Agiralioglu, 1997). Different from uniform flow is non-uniform flow, which can be further divided for both gradually varied flow and rapidly varied unsteady flows, and the same general rules for analysis apply as for steady flow. Flow zones can be viewed as under the 1-D flow assumption; thus, the method of analysis for steady and unsteady flow is the same in this respect.

Based on Saint-Venant equation, the solution scheme of the steady or unsteady flow equations depends on the scheme of its numerical solution (Cunnane, 1988; Ren and Cheng, 2003). In this study, the flow routing process of backwater evolution during a flood event is viewed as one dimensional unsteady flow described with the Saint-Venant equation based on equations of continuity and momentum as below,

$$\begin{cases} \frac{\partial Q}{\partial x} + B\frac{\partial Z}{\partial t} = q_L \\ \frac{\partial Q}{\partial t} + 2v\frac{\partial Q}{\partial x} + (gA - BV^2)\frac{\partial Z}{\partial x} - V^2\frac{\partial A}{\partial x}\Big|_z + g\frac{n_m Q|Q|}{AR_h^{4/3}} = 0 \end{cases} \quad (1)$$

where Q is flood discharge (m^3/s), x is the coordinate horizontal in flow direction, B is the velocity of propagation of the kinematic wave (m/s), Z is water level (m), q_L is the lateral inflow per unit time per unit channel length (m^2/s), t is the time (s), V is flood flow velocity (m/s); g is acceleration due to gravity (m/s^2), A is cross-sectional area of the flow (m^2); R_h is the hydraulic radius (m), n_m is Manning roughness coefficient.

The friction slope S_f is approximated by Manning's equation (Keskin and Agiralioglu, 1997):

$$\begin{cases} S_f = \frac{n_m^2 V|V|}{y^{4/3}} \\ V = \frac{1}{n_m} R_h^{2/3} S_f^{1/2} \end{cases} \quad (2)$$

where S_f is the friction slope, n_m is the Manning's roughness coefficient, R_h is the hydraulic radius (m), and $V|V|$ replaces V^2 to account for the possibility of flow reversal.

Supposing that at time t at the ith reach the channel roughness coefficient is n_i^t, the estimated channel roughness changes at time $\Delta t + t$ due to sediment variation (ΔV_i). This can be described as below (Keskin and Agiralioglu, 1997; Ren and Cheng, 2003):

$$\begin{cases} n_i^{t+\Delta t} = n_i^t - C_n \cdot \frac{\Delta S_i}{\Delta t} \\ n_i^{t+\Delta t} = \begin{cases} 0.5n_i^{t=0}, & n_i^{t+\Delta t} < 0.5n_i^{t=0} \\ 1.5n_i^{t=0}, & n_i^{t+\Delta t} > 1.5n_i^{t=0} \end{cases} \end{cases} \quad (3)$$

where C_n is adaptable empirical coefficient, ΔV is sediment variation and is marked as a positive value when the channel bed is silted and as a negative value when it is scoured (10^9 m^3), Δt is the time change from the previous time step to the present; $n_i^{t=0}$ is the initial value of the channel roughness coefficient at the ith reach, and is defined through field work.

We use the Preissmann three-point implicit scheme (He et al., 2006) to solve the channel flow equations and avoid the disturbing effect of the numerical diffusion on the results of modelling. The flow domain is divided into a number of flow reaches. Accordingly, for a point like 'p' located in a rectangular grid, the average values and derivatives are given by

$$\begin{cases} \frac{\partial f}{\partial x} \approx \frac{\theta(f_{i+1}^{j+1} - f_i^{j+1}) + (1-\theta)(f_{i+1}^j - f_i^j)}{\Delta x_i} \\ \frac{\partial f}{\partial x} \approx \frac{f_{i+1}^{j+1} + f_i^{j+1} - f_{i+1}^j}{2\Delta t} \end{cases} \quad (4)$$

where f is the function of Q, Z, A, V. The subscript of f is the identity of different river reaches; the superscript of f depicts different time periods. is the time weighting coefficient. Δx_i is the length of the ith reach in a river. On substituting the average values in Eq. (1) for the appropriate items in Eq. (4), the following equations are obtained:

$$\begin{cases} -Q_{i-1}^{j+1} + Q_i^j + C_i Z_{i-1}^j + G_i Z_i^{j+1} = D_i \\ E_i Q_{i-1}^{j+1} + G_i Q_i^{j+1} - F_i Z_{i-1}^{j+1} + F_i Z_i^{j+1} = \varphi_i \end{cases} \quad (5)$$

where

$$\begin{aligned} C_i &= \frac{\Delta x_i B_{ij-1/2}}{2\theta\Delta t} \\ D_i &= \frac{1-\theta}{\theta}(Q_{i-1}^j - Q_i^j) + C_i(Z_{i-1}^j + Z_i^j) \\ E_i &= \frac{\Delta x_i}{2\theta\Delta t} - 2V_{i-1/2}^j + \frac{g}{2\theta}\left(\frac{n^2}{R^{1.33}}\right)_i^j |V_{i-1}^j|\Delta x_i \\ F_i &= (gA - BV^2)_{i-1/2}^j \\ \phi_i &= \frac{\Delta x_i}{2\theta\Delta t}(Q_{i-1}^j + Q_i^j) + \frac{2(1-\theta)}{\theta}V_{i-1/2}^j(Q_{i-1}^j - Q_i^j) \\ &\quad + \frac{1-\theta}{\theta}(gA - BV^2)_{i-1/2}^j(Z_{i-1}^j - Z_i^j) \\ &\quad + \frac{\Delta x_i}{\theta}\left(V^2\frac{\partial A}{\partial X}\Big|_Z\right)_{i-1/2}^j \end{aligned} \quad (6)$$

The approaching method was used to estimate flood influence on kinematic wave propagation based on the upper boundary conditions of flood discharge.

Suppose that $\hat{y}$ is an unknown vector at the time of $n+1$, then the general form of Eq. (5) can be represented as

$$\hat{y}_i = F(\hat{y}_{i-1}) \quad (7)$$

where the subscripts i and $i+1$ are times of iterative computation. This iterative computation process is achieved by

$$\hat{y}_{i+1} = \omega\hat{y}_i + (1-\omega)\hat{y}_{i-1} \quad (8)$$

and ends up in case of

$$\max|\hat{y}_i - \hat{y}_{i-1}| < \delta \quad (9)$$

where δ is the value of the control parameter and ω is the lax factor. In iteration, the value of previous time step is viewed as the initial value in the next time step.

Boundary conditions are key factors in computation of hydrological modelling. Based on former studies (Mosselman, 1995; Keskin and Agiralioglu, 1997; Ren and Cheng, 2003), we develop three computation schemes to simulate the complicated flood flow evolution according to the complex flood flow situation in the middle Yellow River: a simple scheme for single main channel with no tributary and backwater, an improved scheme for convergent or divergent flows at the confluence (Weihe River and Luohe River,

Weihe River and middle Yellow River), and an improved scheme for bidirectional flows (Fig. 2).

Simple boundary scheme for single main channel

If there are no tributaries and backwater in a single channel, then the boundary condition of Eq. (1) is defined as below:

$$\begin{cases} Q_1^{n+1} = Q_1 \cdot t_{n+1} \\ Z_N^{n+1} = Z_N \cdot t_{n+1} \end{cases} \tag{10}$$

where Q_1^{n+1} and Z_N^{n+1} are the flood discharge and the water level at the nth time step, Q_1 and Z_N are the initial flood flow discharge and water level, t_{n+1} is the time step at $n+1$. Eq. (10) is used as the boundary conditions, since it describes the relationship between initial status and flood discharges and water levels in next time interval from upstream to downstream. The approaching method is used to estimate backwater evolution processes during flood events based on upper boundary conditions.

$$\begin{cases} Z_i^{n+1} = H_i Z_{i+1}^{n+1} + I_i \\ Q_{i+1}^{n+1} = F_{i+1} Z_{i+1}^{n+1} + G_{i+1} \end{cases} \quad (i = 1, 2, \ldots, N-1) \tag{11}$$

where H_i, I_i, F_{i+1}, G_{i+1} are approaching coefficients, and initial values are defined as $F_1 = 0$, $G_1 = Q_1 \cdot t_{n+1}$. By using these approaching function and boundaries, we can calculate flood water levels and discharge in the main channel where there are no tributaries and backwater.

Improved boundary scheme for convergent and divergent flow

Two assumptions are proposed for the situation when there is a slight amount of flood flow backwater at the confluence between the Weihe River and the Luohe River. First, we neglect the resistance influence of backwater on the boundary conditions. Second, we assume that convergent flow discharge has a positive value (from the Luohe River to the Weihe River), and divergent flow discharge has a negative value (from the Weihe River to the Luohe River). As is shown in Fig. 2A, we define the boundary condition as

$$\begin{cases} Q_{a1}^{n+1} + Q_{b1}^{n+1} = Q_{c1}^{n+1} \\ Z_{a1}^{n+1} + \frac{1}{2g}\left(\frac{Q_{a1}^{n+1}}{A_{a1}}\right)^2 = Z_{c1}^{n+1} + \frac{1}{2g}\left(\frac{Q_{c1}^{n+1}}{A_{c1}}\right)^2 \\ Z_{b1}^{n+1} + \frac{1}{2g}\left(\frac{Q_{b1}^{n+1}}{A_{b1}}\right)^2 = Z_{c1}^{n+1} \cdot \frac{1}{2g}\left(\frac{Q_{c1}^{n+1}}{A_{c1}}\right)^2 \end{cases} \tag{12}$$

From Eq. (5), we can relate flood discharge with water level at cross-section a and b as below,

$$\begin{cases} Q_{a1}^{n+1} = F_{a1} Z_{a1}^{n+1} + G_{a1} \\ Q_{b1}^{n+1} = F_{b1} Z_{b1}^{n+1} + G_{b1} \end{cases} \tag{13}$$

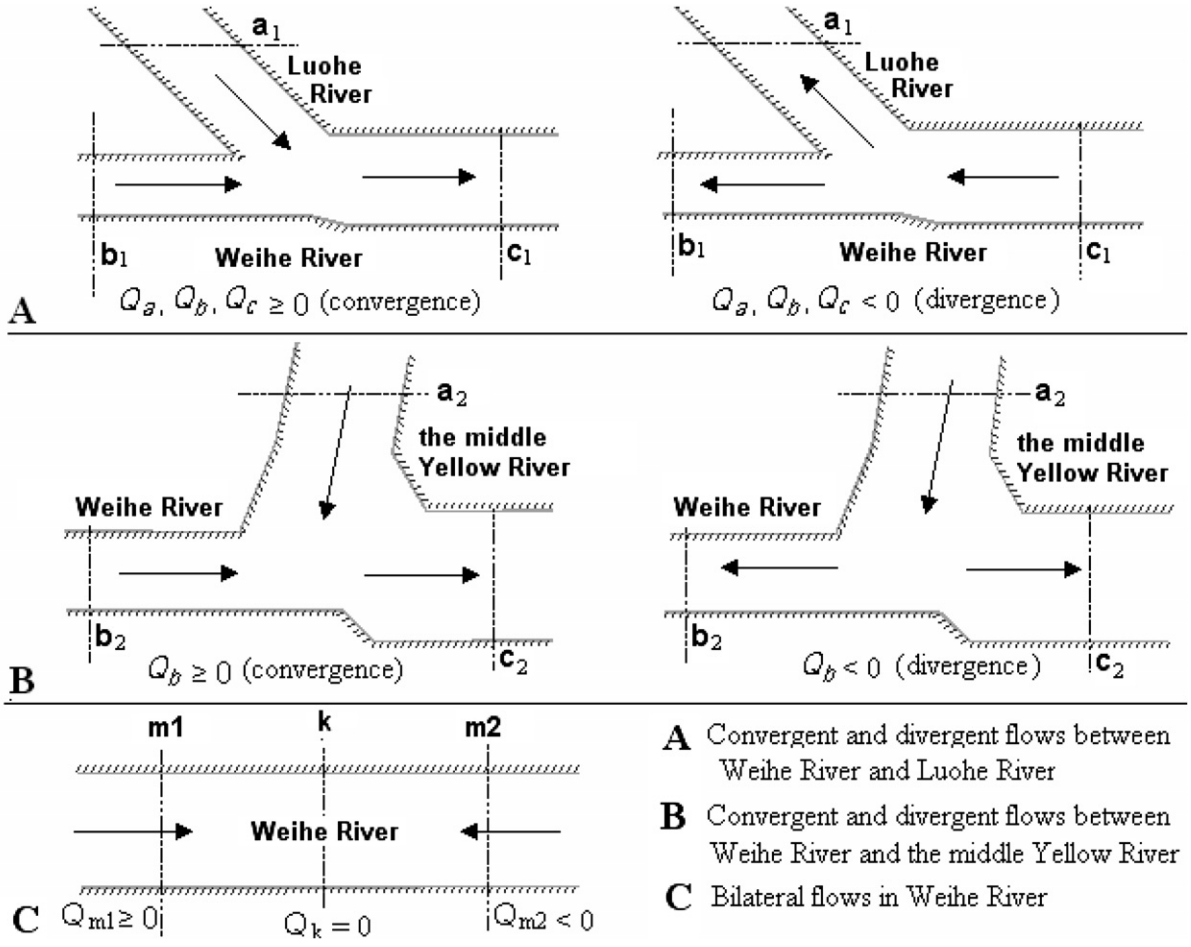

Figure 2 Computational schemes of flood routing of backwater in the middle Yellow River basin.

Therefore, Eq. (12) may be written as

$$\begin{cases} Q_{c1}^{n+1} = F_{c1} Z_{c1}^{n+1} + G_{1c} \\ Z_{a1}^{n+1} = Z_{c1}^{n+1} + \Delta Z_{a1c1}^{n+1} \\ Z_{b1}^{n+1} = Z_{c1}^{n+1} + \Delta Z_{b1c1}^{n+1} \end{cases} \tag{14}$$

where

$$\begin{cases} \Delta Z_{a1c1}^{n+1} = \frac{1}{2g}\left[\left(\frac{Q_{c1}^{n+1}}{A_{c1}}\right)^2 - \left(\frac{Q_{a1}^{n+1}}{A_{a1}}\right)^2\right] \\ \Delta Z_{b1c1}^{n+1} = \frac{1}{2g}\left[\left(\frac{Q_{c1}^{n+1}}{A_{c1}}\right)^2 - \left(\frac{Q_{b1}^{n+1}}{A_{b1}}\right)^2\right] \end{cases} \tag{15}$$

The approaching coefficients are defined as

$$\begin{cases} F_{c1} = F_{a1} + F_{b1} \\ G_{c1} = G_{a1} + G_{b1} + F_{a1} \cdot \Delta Z_{a1c1}^{n+1} + F_{b1} \cdot \Delta Z_{b1c1}^{n+1} \end{cases} \tag{16}$$

When the flood water level at cross-section c_1 (Z_{c1}, at the convergence) is obtained, we can calculate the flow discharge at cross-section c_1 (Q_{c1}), and water levels at cross-section a_1 (Z_{a1}, in the Luohe River) and b_1 (Z_{b1}, in the Weihe River).

At the confluence of the Weihe River and the middle Yellow River, there are huge amounts of flood flow convergence, divergence and backwater, and resistance influence of backwater cannot be neglected. For the purpose of the simulation, we assume that convergent flood flow discharge has a positive value (Fig. 2B, from Weihe River to the middle Yellow River), and that divergent flood flow discharge has a negative value (from the middle Yellow River to the Weihe River). Models are constructed to simulate these two different flood flow situations. The boundary condition from the middle Yellow River to the Weihe River is defined as

$$\begin{cases} Q_{a2}^{n+1} + Q_{b2}^{n+1} = Q_{c2}^{n+1} \\ Z_{a2}^{n+1} + \frac{\left(U_{a2}^{n+1}\right)^2}{2g} = Z_{c2} + (1 + \xi_{a2c2}) \frac{(U_{c2}^{n+1})^2}{2g} \\ \qquad + \frac{\Delta x_{a2c2}}{2}\left(\frac{n_{a2}^2 (U_{a2}^{n+1})^2}{R_{a2}^{4/3}} + \frac{n_{c2}^2 (U_{c2}^{n+1})^2}{R_{c2}^{4/3}}\right) \\ Z_{b2}^{n+1} + \frac{(U_{b2}^{n+1})^2}{2g} = Z_{c2} + (1 + \xi_{b2c2}) \frac{(U_{c2}^{n+1})^2}{2g} \\ \qquad + \frac{\Delta x_{b2c2}}{2}\left(\frac{n_{b2}^2 (U_{a2}^{n+1})^2}{R_{b2}^{4/3}} + \frac{n_{c2}^2 (U_{c2}^{n+1})^2}{R_{c2}^{4/3}}\right) \end{cases} \tag{17}$$

where U_{a2}, U_{b2} and U_{c2} are average flood flow velocities at cross-sections of the middle Yellow River (cross-section a_2, main channel), the Weihe River (cross-section b_2, tributary), and the convergence (cross-section c_2); R_{a2}, R_{b2} and R_{c2} are hydraulic radii at each cross-section (cross-section a_2, b_2 and c_2); n_{a2}, n_{b2} and n_{c2} are Manning roughness coefficients at each cross-section (cross-section a_2, b_2 and c_2); ΔX_{a2c2} and ΔX_{b2c2} are distances from the main channel (cross-section a_2, the middle Yellow River) to the confluence section (cross-section c_2), and from the tributary channel (cross-section b_2, the Weihe River) to the confluence section (cross-section c_2); ζ_{a2c2}, ζ_{b2c2} are regional resistant coefficients from the main channel (cross-section a_2, the middle Yellow River) to the confluence section (cross-section c_2), and from the tributary channel (cross-section b_2, the Weihe River) to the confluence section (cross-section c_2). The rest of the parameters have the same physical meaning as indicated above. Based on the boundary conditions of Eq. (17), flood discharge and water levels from the middle Yellow River to the Weihe River can be computed.

The boundary condition from the Weihe River to the middle Yellow River is defined as

$$\begin{cases} Q_{a2}^{n+1} + Q_{b2}^{n+1} = Q_{c2}^{n+1} \\ Z_{a2}^{n+1} + \frac{(U_{a2}^{n+1})^2}{2g} = Z_{c2} + (1 + \xi_{a2c2}) \frac{(U_{c2}^{n+1})^2}{2g} \\ \qquad + \frac{\Delta x_{a2c2}}{2}\left(\frac{n_{a2}^2 (U_{a2}^{n+1})^2}{R_{a2}^{4/3}} + \frac{n_{c2}^2 (U_{c2}^{n+1})^2}{R_{c2}^{4/3}}\right) \\ Z_{a2}^{n+1} + \frac{(U_{a2}^{n+1})^2}{2g} = Z_{b2} + (1 + \xi_{a2b2}) \frac{(U_{b2}^{n+1})^2}{2g} \\ \qquad + \frac{\Delta x_{a2b2}}{2}\left(\frac{n_{a2}^2 (U_{a2}^{n+1})^2}{R_{a2}^{4/3}} + \frac{n_{b2}^2 (U_{b2}^{n+1})^2}{R_{b2}^{4/3}}\right) \end{cases} \tag{18}$$

where ΔX_{a2b2} is the distance from divergence (cross-section a_2) to the tributary channel (cross-section b_2, the Weihe River); ζ_{a2b2}, is the regional resistant coefficient from the main channel (cross-section a_2, the middle Yellow River) to the tributary channel (cross-section b_2, Weihe River). Using Eq. (18), flood discharge and water levels from the Weihe River to the middle Yellow River can be computed.

Improved boundary scheme for bidirectional flow

The improved boundary scheme for bidirectional flow focused on modelling two flood flows of similar magnitudes travelling in opposite directions. Other cases of bidirectional flows of different magnitudes have been considered in the improved boundary scheme for convergent and divergent flows. The type of backwater in bidirectional flood flow is relatively rare. Bidirectional flood flows occur when backwater flows back from the middle Yellow River to the Weihe River (Fig. 2C). When two flood flows in opposite directions meet, a zero flood discharge will occur. Therefore, we can define that as,

$$\begin{cases} Q_{m1}^{n+1} = Q_{m2}^{n+1} = 0 \\ Z_{m1}^{n+1} = Z_{m2}^{n+1} \end{cases} \tag{19}$$

and approaching coefficients in Eq. (5) can be calculated from Eq. (19). However, the confluence cross-section of the two bidirectional flows is relatively difficult to locate as it relates with the state of ebb-and-flow of the two flood flows, and varies with time. Therefore, we use an explicit difference solution to solve the problem and to calculate flood flow parameters at time step of $n\Delta t$.

The computation time interval (Δt) is one of the key parameters in our model simulation. Two factors are important in choosing the time step in the computation. First, the interval should be short enough to accurately describe the rise and fall of the hydrographs being routed. Second, the computation interval should be adjusted by variations of hydraulic features, such as boundary conditions. By considering the propagation of peak discharge and water level, we define time interval (Δt) and distance interval (Δx) by the functions described as below

$$\begin{cases} \Delta t = 0.5 \quad t \leqslant \tau - 0.5 \\ \Delta t = t_p/20 \quad \tau - 0.5 \leqslant t \leqslant \tau + 2\tau \\ \Delta t = T_p/20 \quad t \geqslant \tau + 2t_p \\ \Delta x = c_f \cdot \Delta t \end{cases} \tag{20}$$

where Δt is the time interval (h), t_p is the time of first occurrence of peak discharge (h), T_p is the time of peak discharge occurrence in selected cross-section (h), τ is the time of peak discharge occurrence in the outlet (h), C_f is the celerity of flood wave propagation (m/s), and Δt is the distance interval (m). The time intervals range from 0.5 to 1 h. The distance intervals range from 3.1 to 5.5 km for 13 reaches. The ratios of time interval to distance interval ($\Delta t/\Delta x$) are between 3.5 and 6.3.

Variations of the roughness friction parameter n_m in Eq. (2) increase in relation to the highest wave number. That might result in a wave speed greater than in reality. In these situations, it usually causes computational instabilities. This numerical scheme needs a dissipation mechanism in order to eliminate accumulation of dispersion errors. Therefore, it is advisable to increase the coefficient of time weighting parameter, θ. Time coefficients are usually defined as 0.3–0.65 depending on the situation of roughness coefficient. After a series of adaptations, C_n in Eq. (3) ranges from 0.4 to 0.6. Considering the complex of land surface conditions in the middle Yellow River, we define θ as 0.6 and the roughness coefficient as 0.032. Estimation of channel roughness in flood routing is based on Eq. (3). To calculate the channel roughness during different routing times, we need to know the initial roughness. The initial roughness is defined by following steps. First, after accounting for flood water levels at different discharges for each gauge cross-section, we can get iso-surfaces of those discharges. Second, we can get initial roughness values when the simulated water levels are compared with gauged water levels by adapting roughness values (Table 1). Some of these parameters are determined based on the experience of experts combined with referencing to historic observation records and literatures from USGS.

Table 1 Channel configurations used in the study

Parameters				The Luohe River	The Weihe River	The small north mainstream (downstream of the middle Yellow River)
Channel type				Rectangular	Rectangular	Rectangular
Channel length (km)				154	155	132.5
Average channel width (m)		1952–1964		80–100	150–180	180–240
		1964–1986		90–120	180–230	200–240
		1987–2003		100–150	200–250	210–250
Average channel slope (%)		1952–1964		3.5	3.2	2.8
		1964–1986		2.7	2.3	2.5
		1987–2003		2.2	1.4	2.4
Initial Manning's roughness	1952–1964	Discharge (m^3/s)	Manning's roughness	0.15	0.14	0.19
		100	0.017			
		500	0.016			
		1000	0.016			
		2000	0.015			
		4000	0.014			
		8000	0.012			
		>10000	0.010			
	1964–1986	100	0.022	0.17	0.21	0.20
		500	0.021			
		1000	0.020			
		2000	0.019			
		4000	0.018			
		8000	0.017			
		>10000	0.015			
	1987–2003	100	0.028	0.23	0.31	0.28
		500	0.027			
		1000	0.025			
		2000	0.025			
		4000	0.024			
		8000	0.023			
		>10000	0.021			
Variable cross-section interval (Δx, km)				3.1	5.5	3.5
Grid element number				163650	294600	278250
Ratio of spatial–temporal interval ($\Delta x/\Delta t$)				3.5	6.3	4.2

In the study area, two upstream channels meet and form a larger channel at the junction point (Fig. 1). According to the geometry, the values of each parameter associated with the routing are functions with time because of channel morphology changes. The physical setups of the model are shown in Table 1. The modelling works on each of the total of 736 500 elements of the river discretized with lengths on the basis of DEM resolution (30 m). Other discretized schemes were described in the Methodology section. For example, the time intervals range from 0.5 to 1 h, the distance intervals range from 3.1 to 5.5 km for 13 reaches or the ratios of time interval to distance interval ($\Delta t/\Delta x$) are between 3.5 and 6.3.

Calibration and validation of the model are performed through four flood events (July 27—31, 1962; June 25, 1968; August 28, 1970; September 25—October 5, 1983). Parameter values are adjusted from the initial estimates given in the model within the acceptable ranges to achieve the desired proportion after simulation by using the trial-and-error method. The model was calibrated by considering all the possible combinations of parameters. This procedure is repeated until optimal parameter values are found by comparing the simulated and observed rainstorm—flood event data. Coefficient of Model Efficiency (CME, Nash and Sutcliffe, 1970) and Root Mean Square Error (RMSE) are used to evaluate model efficiency.

Flood contribution index

An index was developed to evaluate the contribution of river bed slope, channel roughness, and water volume amount to flood wave propagation. This contribution index, *CI*, can be represented as

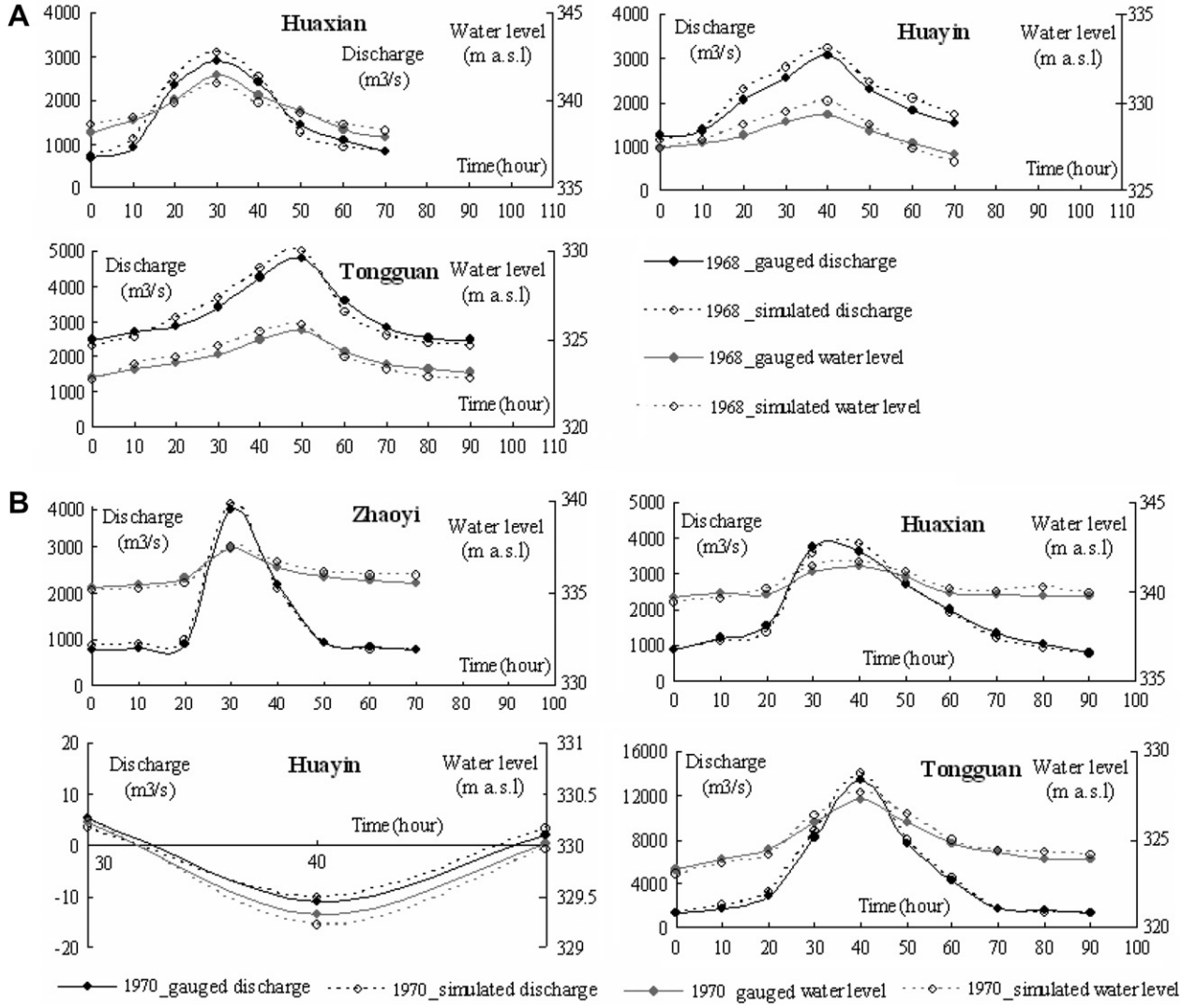

Figure 3 Calibrating simulation of the flood routing model in the middle Yellow River basin for the floods of July 27—31, 1962; June 25, 1968; August 28, 1970; September 25—October 5, 1983. (A) Model calibration for unilateral flow routing in the Weihe River (simple scheme; Juny 25, 1968 (m a.s.l)). (B) Model calibration for flood routing in the Weihe/Luohe Rivers (improved boundary scheme; August 28, 1970). (C) Model calibration for flood routing in the Weihe/middle Yellow Rivers (improved boundary scheme; July 27—31, 1962). (D) Model calibration for bilateral flow in the Weihe River (improved boundary scheme; September 25—October 5, 1983).

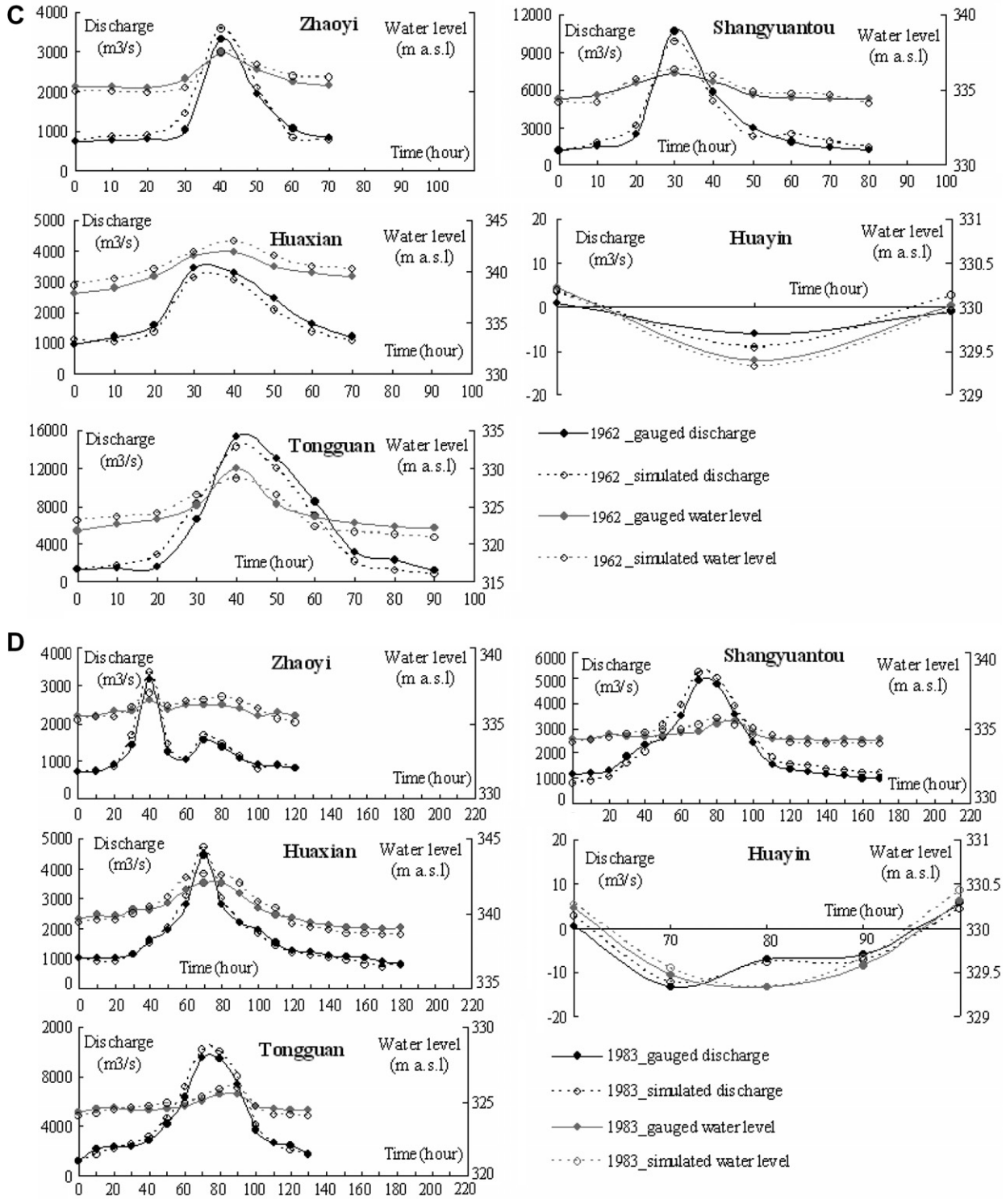

Figure 3 (*continued*)

$$CI = P_j \Big/ \sum_{i=1}^{n} P_i$$

where *CI* value is between 0 and 1. The higher the index value the greater the contribution of a given parameter to flood wave propagation. P_j is simulated value of a certain variable (such as river bed slope, channel roughness, and water volume) in a given scenario (such as roughness of 1962 and 2003, river bed slope of 1962 and 2003); $\sum P_i$ is the total value of a certain variable in all designed scenarios.

Results and discussion

Simulation of three computational boundary schemes in flood routing

Results of simulating flood routing processes for the three computational schemes are presented below. Before analyzing the modelling results, we first describe calibration and validation of the model.

Model calibration and validation

The model was calibrated and the results were validated (Fig. 3) with the runoff measured during four flood events (July 27—31, 1962; June 25, 1968; August 28, 1970; September 25—October 5, 1983). The validation was based on measured and estimated discharges and water levels at various stations and flood events. The coefficients of the model efficiency ($-\infty$ < CME < 1; Nash and Sutcliffe, 1970) ranged from 0.83 to 0.91 (Table 2). Root Mean Square Errors (RMSEs) fall within 34.6—39.4 m^3/s for flow discharges, and 0.14—0.29 m for water levels. The measured hydrographs are highly variable in time. In most scenarios, the modelled results consistently matched the measurements performed during all flood events on particular rivers. A major error in simulating runoff corresponded to the duration of peak flows. The model was able to describe the magnitude of backwater generated due to an abrupt fluctuation of boundary conditions with tolerable errors. The boundary conditions for the cross-sections in the Weihe River/the middle Yellow River are the most complex. However, the model performance of simulating flood characteristics on the complex boundary conditions is satisfactory (Fig. 3C). The Coefficients of Model Efficiency (CME) of the modelled discharge and water level are 0.77 and 0.83 for the flood event in July 27—31, 1962. Root Mean Square Errors (RMSE) of discharge and water level are 39.4 (m^3/s) and 0.29 m, respectively.

Simple boundary scheme for single main channel

Results from simulating unilateral flow in the Weihe River for the flood event on July 6—8, 1990 were based on the proposed simple boundary scheme. Hydrographs in the river are relatively simple as there are no tributary flows or backwater in the routing process. Unilateral flow routes along a single channel and usually happens during non-flood seasons or in relatively small flood events (State Flood Control and Drought Relief Headquarters, 1992). Estimated hydrographs of discharge and water level were developed for the gauge cross-sections of Huaxian, Chenchun, and Huayin. Fig. 4 shows the observed hydrographs and simulation results on the basis of a simple boundary scheme for a single main channel. It can be observed that the rising limbs and the recession limbs of the hydrographs have almost the same slopes at successive gauges. This indicates that flood routing along the single channel is mostly dominated by temporal distribution of rainstorms. Importantly, backwater does not exist in this situation. By comparing the observed hydrographs and the simulation results in simple boundary schemes, Table 2 shows model efficiency for single main channel in the event of July 6—8, 1990. Coefficients of Model Efficiency (CME) of discharge and water level are 0.83 and 0.85 (July 27—31, 1962), whereas Root Mean Square Error (RMSE) of discharge and water level are 43.3 m^3/s and 0.21 m (July 27—31, 1962).

Improved boundary scheme for convergent and divergent flow

We adopted the improved boundary scheme for convergent and divergent flow to the river segment from the middle Yellow River to the Weihe River for the flood event in August 3—4, 1977. Backwater in this river segment happens when flood flows from the Weihe to Luohe Rivers converge synchronously, or when a greater flood on the middle Yellow River than that on the Weihe results in flow divergence at the confluence of the Weihe and Louhe Rivers (Fig. 2). Observed hydrographs and simulated results for convergent and divergent flows in the river segment and for the four flood events between 1977 and 2003 are displayed in Fig. 5 (the Weihe and Luohe Rivers) and Fig. 6 (the middle Yellow River and Weihe River). By comparing with the unilateral flood flow, the hydrographs of convergent and divergent flood flows show distinctive behaviours. The rising limbs have much steeper slopes than the recession limbs in the routing process in the Weihe and the middle Yellow Rivers. In the Weihe and Luohe Rivers, the rising limbs have relatively gentler slopes than the recession limbs. The magnitude of backwater in the Weihe River/Luohe River (Fig. 5)

Table 2 Evaluation of the efficiency of the proposed flood routing model based on simulated peak discharges and water levels for seven historical flood waves in the middle Yellow River basin

	Nash—Sutcliffe coefficient		RMSE	
	Flow discharge	Water level	Flow discharge (m^3/s)	Water level (m)
July 27—31, 1962	0.77	0.83	39.4	0.29
June 25, 1968	0.89	0.84	34.6	0.28
August 28, 1970	0.83	0.87	37.7	0.25
August 3—4, 1977	0.80	0.78	47.2	0.26
September 25—October 5,1983	0.91	0.87	37.6	0.14
July 6—8, 1990	0.83	0.85	43.3	0.21
June 6, 1992	0.87	0.83	41.8	0.20
August 25, 2003	0.75	0.79	52.3	0.34

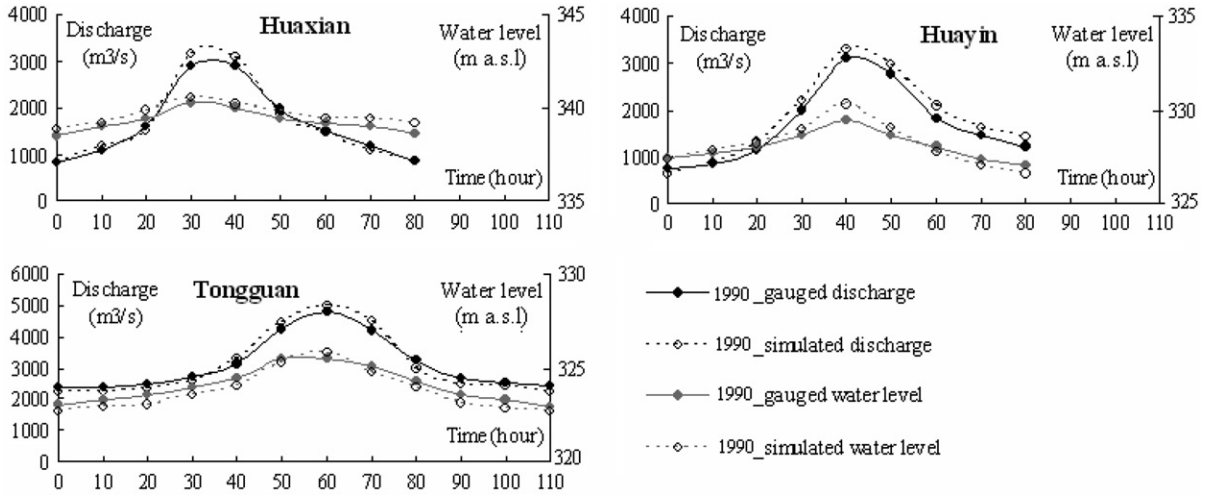

Figure 4 Simulation of unilateral flow (simple boundary scheme for single main channel) in the Weihe River (July 6—8, 1990).

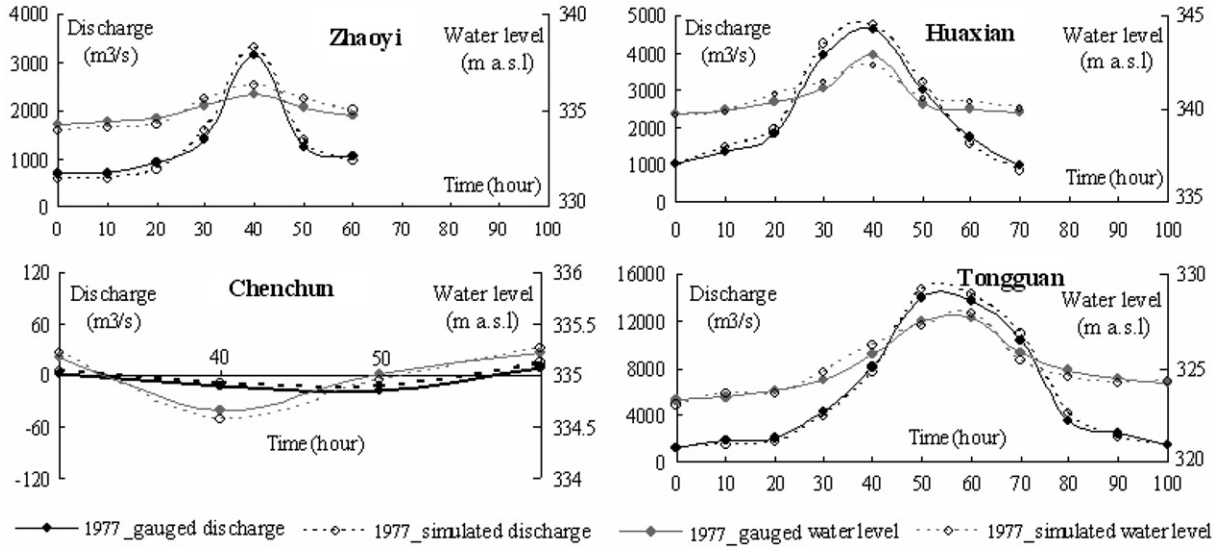

Figure 5 Simulation of flood flow in the Weihe/Luohe Rivers (improved boundary scheme; August 3—4, 1977).

was much smaller than that in Weihe River/the middle Yellow River (Fig. 6), although the backwater in both rivers traced back to Chenchun. At Tongguan fluctuation of flood wave in the Weihe/Louhe Rivers (Fig. 6), occurred more frequently than that in the Weihe/the middle Yellow Rivers due to flood flows (Fig. 5). This phenomenon was due to the greater magnitude of backwater effects displayed in Fig. 6. Model efficiency of evaluating the improved boundary scheme for convergent and divergent flow was summarized in Table 2. Coefficients of Model Efficiency (CME) are 0.80 for the event in 1977 and 0.75 for the event in 2003 for flow discharge, and 0.78 (1977) and 0.79 (2003) for water level. Root Mean Square Errors (RMSE) are 47.2 and 52.3 m^3/s for the flow discharge in 1977 and 2003, and 0.26 and 0.34 m for the water level in 1977 and 2003, respectively.

The analysis of flow routing processes for the four flood events in 1962, 1970, 1977, and 2003 indicates that backwater usually occurred when flow discharges in the main river were greater than that in tributary. For example, the observed peak discharges at Shanyuantou on the middle Yellow River and at Huanxian on the Weihe River amounted to 10,400 and 3750 m^3/s in 1962, to 8140 and 4320 m^3/s in 1970, to 4470 and 9460 m^3/s in 1977 and to 5670 and 4250 m^3/s in 2003. The occurrence of backwater in the Weihe River was based on function (21) by analyzing the relationship between flow discharges and water levels in the Weihe River

$$\begin{cases} S_{DQ-HY} \leqslant 0 \\ Q_{maxTG} \cdot \sqrt{Q_{HX}} \geqslant 25 \\ V_{zTG} \geqslant 0.06 \end{cases} \quad (21)$$

where S_{DQ-HY} is the slope of water level from Diaoqiao to Huayin, Q_{maxTG} is the peak discharge at Tongguan (m^3/s), $\sqrt{Q_{HX}}$ is the daily mean flow discharge in a given year (m^3/s), and V_{zTG} is the rate of water level rise (m/h). The end of backwater reached peak values around the time that

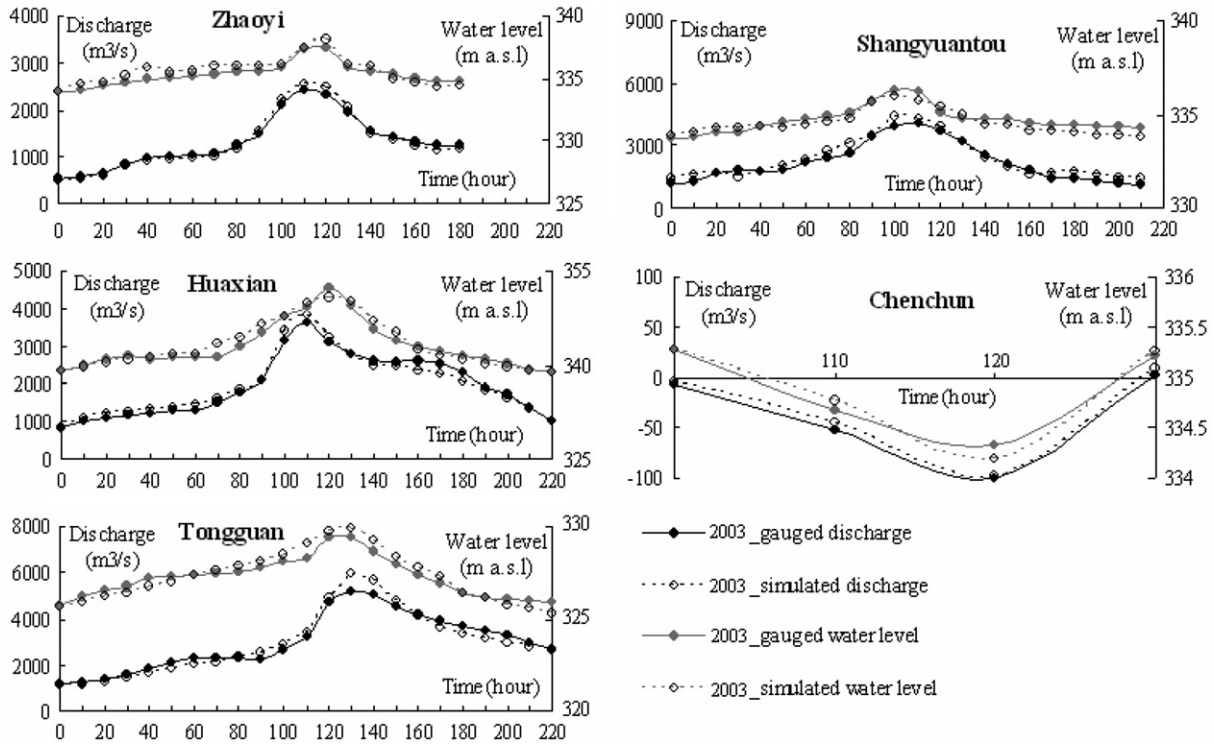

Figure 6 Simulation of flood flow in the Weihe/middle Yellow Rivers (improved boundary scheme; August 25, 2003).

peak flow occurred in Tongguan. For example, backwater occurred 2—3 h earlier in Huanyin (39th hour in 1962) and Chenchun (49th hour in 1977, 133rd hour in 2003) than peak discharge in Tongguan (41st hour in 1962, 52nd hour in 1977, 135th hour in 2003) in 1977 and 2003, respectively. However, the shapes of the hydrographs (both flow discharge

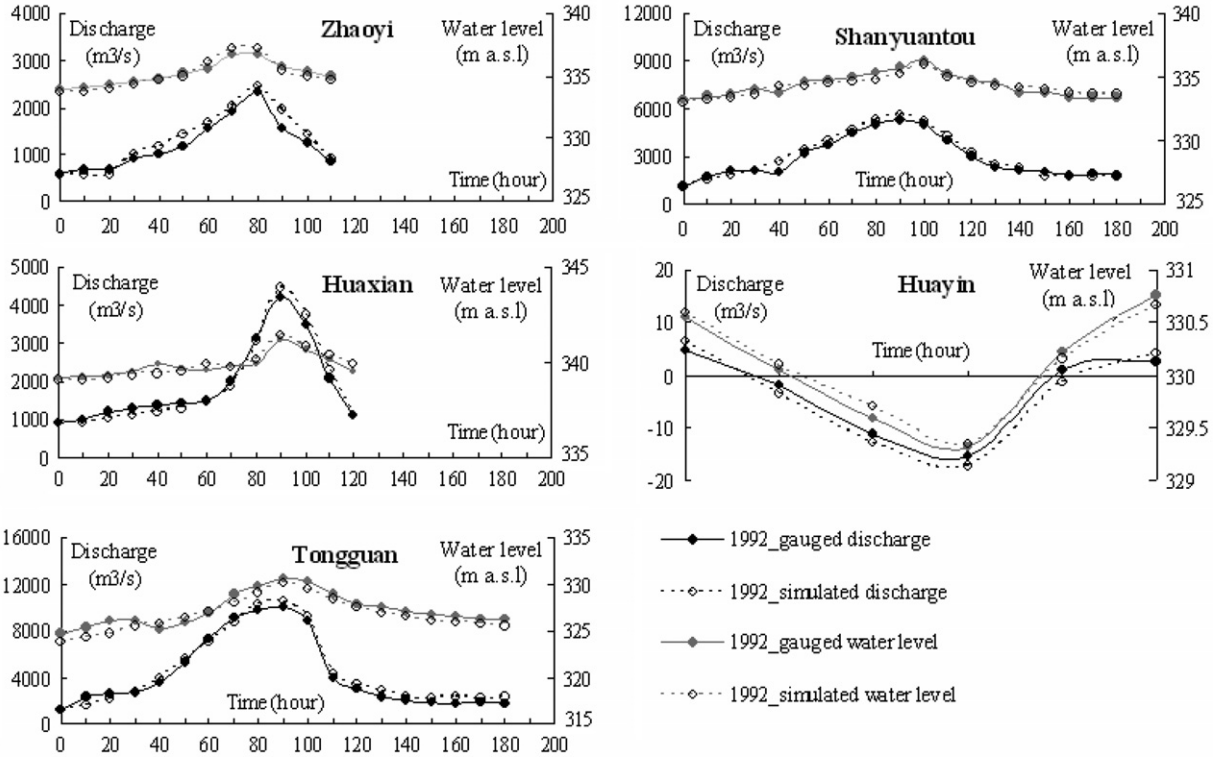

Figure 7 Simulation of bilateral flow in the Weihe River (improved boundary scheme; June 6, 1992).

and water level) at the end of backwater (such as Huayin and Chenchun) were similar to those of the hydrographs in Tongguan.

Improved boundary scheme for bidirectional flow

The results of simulating bidirectional flow in which two floods of similar magnitudes converge in the opposite directions were examined using data from historic flood records. One example of the occurrence of backwater resulting from bidirectional flow was on Jun 6, 1992 when flood water flowed from the middle Yellow River (5200 m^3/s in Shanyuantou) to the Weihe River (4550 m^3/s in Huaxian). Fig. 7 shows the observed hydrographs and simulated results for this event. A magnitude of the backwater resulting from bidirectional flow is relatively small compared with that which occurs when flood flow diverts from the main stream to the tributary. The rising limbs and the recession limbs fluctuated due to the effect of backwater. Table 2 listed model efficiency of improved boundary scheme for bidirectional flow (June 6, 1992). Coefficients of Model Efficiency (CME) of discharge and water level are 0.87 and 0.83 (June 6, 1992), whereas Root Mean Square Errors (RMSE) of discharge and water level are 41.8 m^3/s and 0.20 m (June 6, 1992).

Through the analysis of seven historical flood events in the middle Yellow River basin (1962, 1970, 1977, 1983, 1990, 1992, and 2003), the model identified that the shape of the flood hydrographs changed over time from high and thin to low and wide (Figs. 3–7). These changes were accompanied by a delayed occurrence and an extended duration of peak flow of progressively later floods. These trends were intensified from the early 1980s. For example, flood hydrographs at the Huaxian gauge demonstrate that peak discharges, water levels, flood durations and backwater conditions changed considerably between 1962 and 2003. Peak discharges of the floods of 1962 (3750 m^3/s) and 2003 (3595 m^3/s) were similar. However, since 1962 peak water level raised by 8.8 m (333.2 m a.s.l. in 1962 and 342 m a.s.l. in 2003), the occurrence of peak flow delayed by about 99 h (10th hour in 1962 and 109th hour in 2003), and flood duration (with threshold discharge being 950 m^3/s) extended by 177 h (42 h in 1962 and 219 h in 2003). In turn, flood hydrographs at the Tongguan gauge show that the peak discharge of the 2003 flood (5200 m^3/s) amounted to only one-third of that in 1962 (15,300 m^3/s) but flood duration (with threshold discharge being 950 m^3/s) extended by 137 h (89 h in 1962 and 226 h in 2003). Backwater traced back for 23 km (Chenhun in 1962 and Huanyin in 2003), and peak discharge of the backwater increased by 95 m^3/s (−18 m^3/s in 1962 and −103 m^3/s in 2003). From the above information it is evident that flood flow propagation in the middle Yellow River basin experienced significant change during the study period.

Effects of boundary conditions on flood routing

Boundary conditions of river flows refer to geometric features and surface roughness of the river channel at given water volumes. We analyzed the effects of boundary conditions on flood routing processes based on the case of the lower Weihe River channel. This river channel has been shaped by the interaction between fluvial erosion and deposition, and channel morphology for centuries (State Flood Control and Drought Relief Headquarters, 1992). After the construction of the Sanmenxia Reservoir in the 1960s, fluvial deposition became the dominant factor for alteration of the channel morphology in the lower Weihe River (He et al., 2006). In return, the altered river channel boundary conditions imposed significant impacts on flood routing, especially for backwater (Table 1).

Table 3 presents the combinations of simulating flood routing with the features of backwater under different scenarios. The results identified those parameters of the model which affected flood routing in the lower Weihe River. These parameters are river bed slope, channel roughness, and water volume. The simulation scenarios were considered in two categories. In the first category, the channel roughness and river bed slope of 1962 and 2003 are combined with the boundary conditions of 1977 (Table 3; For example, water volume 1B-roughness of 1962 and river bed slope of 1962, r1962s1962; 1C-roughness of 1962 and river bed slope of 2003, r1962s2003; 1D-roughness of 2003 and river bed slope of 1962, r2003s1962; 1E-roughness of 2003 and river bed slope of 2003, r2003s2003). In the second category, the channel roughness and river bed slope of 1962 and 1977 are combined with boundary conditions of 2003 (Table 3; 2B-channel roughness of 1962 and river bed slope

Table 3 Designed scenarios of simulating flood routing in the lower Weihe River for combined initial boundary conditions

Types	Combinations	Initial discharge	Initial roughness	Initial slope
1A	Gauged, r1977s1977	1977	1977	1977
1B	r1962s1962		1962	1962
1C	r1962s2003		1962	2003
1D	r2003s1962		2003	1962
1E	r2003s2003		2003	2003
2A	Gauged, r2003s2003	2003	2003	2003
2B	r1962s1962		1962	1962
2C	r1962s1977		1962	1977
2D	r1977s1962		1977	1962
2E	1977s1977		1977	1977

r is river bed roughness, s is river bed slope.

of 1962, r1962s1962; 2C-channel roughness of 1962 and river bed slope of 1977, r1962s1977; 2D-channel roughness of 1977 and river bed slope of 1962, r1977s1962; 2E-channel roughness of 1977 and river bed slope of 2003, r1977s2003). Two of the considered combinations of the model parameters, namely 1A (channel roughness and river bed slope of 1977, r1977s1977) and 2A (channel roughness and river bed slope of 2003, r2003s2003) represent conditions for the actually observed flows in the routing process.

By conducting simulations of flood routing on the basis of the two above scenarios, we investigated the effects of river bed slope, channel roughness, and water volume on flood routing in the lower Weihe River (Figs. 8 and 9). Below we discuss the simulation results separately for each of the boundary conditions.

Effects of different river bed slopes on backwater routing

Fig. 8 shows that with flood wave volume and channel roughness of 1997, a reduction in river slope from 3.2‰ (r1962s1962) to 2.0‰ (r1962s2003) would decrease peak discharge at Tongguan by 1480 m^3/s (14,560 m^3/s of r1962s1962 and 13,080 m^3/s of r1962s2003), delay the occurrence of peak flow by 1 h (48 h of r1962s1962 and 49 h of r1962s2003), extended flood duration by 8 h (90 h of r1962s1962, and 98 h of r1962s2003) and raise peak water level by 0.5 m (327.5 m a.s.l. of r1962s1962 and 328 m a.s.l. of r1962s2003). However, under both boundary conditions, backwater would trace back to Chenchun. Fig. 9A and B shows that backwater flow at Chenchun would present different behaviours. Peak discharge of backwater would increase by 7 m^3/s (−8 m^3/s of r1962s1962, and −15 m^3/s of r1962s2003), and would occur 3 h earlier (45 h of r1962s1962 and 42 h of r1962s2003), backwater duration would increase by 4 h (8 h of r1962s1962, and 12 h of r1962s2003), and water level would be higher by 0.2 m (328.5 m a.s.l. of r1962s1962 and 328.7 m a.s.l. of r1962s2003).

Effects of different river channel roughness on backwater routing

The effect of different river channel roughness on flood routing was simulated under the same conditions of flood wave volume and river bed slope. Fig. 8 shows that with flood wave volume and river bed slope of 1977, the increase in channel roughness (Manning coefficient) from 0.014 (r1962s1962) to 0.025 (r2003s1962) would decrease peak discharge at Tongguan by 1300 m^3/s (14,560 m^3/s of r1962s1962 and 13,260 m^3/s of r2003s1962), delay the occurrence of peak flow by 4 h (48 h of r1962s1962 and 52 h of r2003s1962), extend flood duration by 11 h (90 h of r1962s1962, and 101 r2003s1962), and raise peak water level by 0.8 m (327.5 m a.s.l. of r1962s1962 and 328.3 m a.s.l. of r2003s1962). Again, under both boundary conditions, backwater would trace back to Chenchun (Fig. 9A and B). Flood routing of backwater at Chenchun shows that with the increase in the channel roughness of the lower Weihe River, peak discharge would increase by 2 m^3/s (−8 m^3/s of r1962s1962, and −10 m^3/s of r2003s1962) and would occur 2 h earlier (45 h of r1962s1962 and 43 h of r2003s1962), backwater duration would increase by 3 h (8 h of r1962s1962, and 11 h of r2003s1962), and water level would rise by 0.4 m (328.5 m a.s.l. of r1962s1962 and 328.9 m a.s.l. of r2003s1962).

Effects of different water volume on backwater routing

Effects of different water volume in flood routing were simulated under the same conditions of channel roughness and river bed slope (Figs. 8 and 9). Firstly, Fig. 8 shows that with

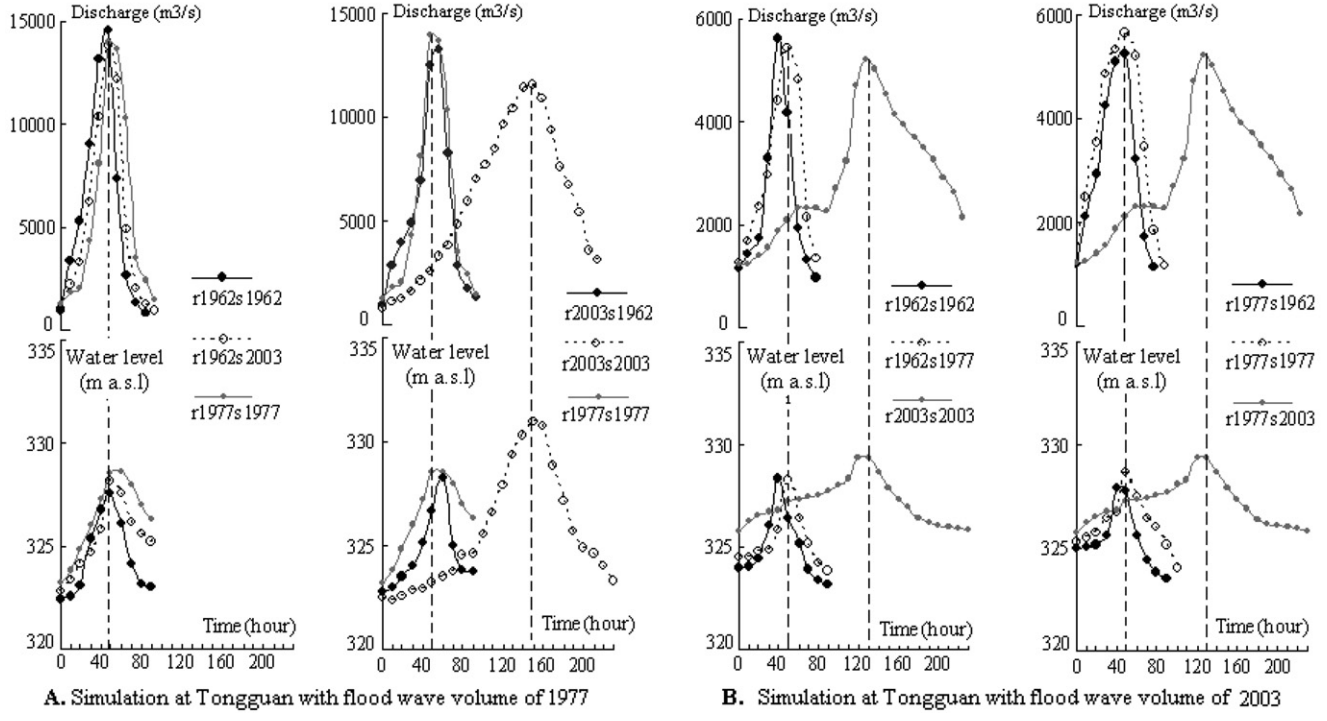

Figure 8 Simulated flood routing under combined scenarios at Tongguan on the Weihe River.

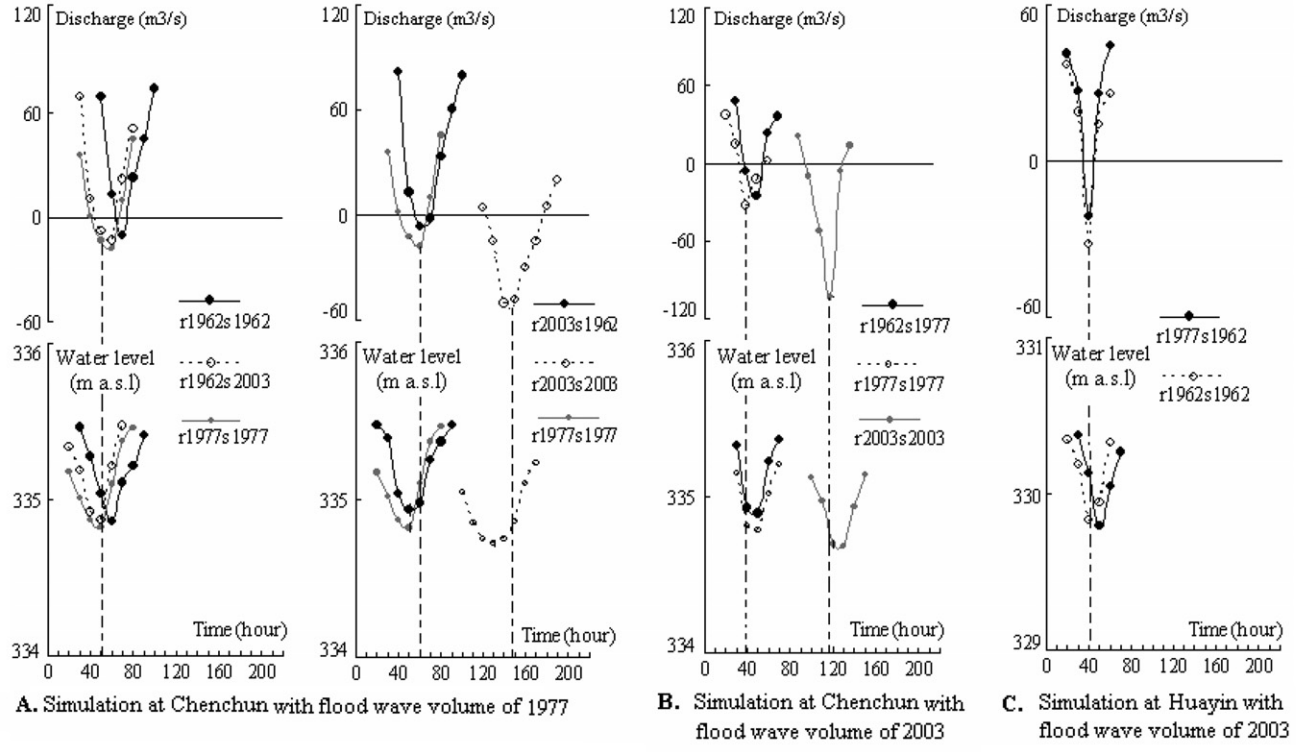

Figure 9 Simulated flood routing under designed scenarios at Chenchun and Huayin on the Weihe River.

channel roughness and river bed slope of 1962, a reduction in flood wave volume from the one typically of the 1977 flood (caused by 843 mm of precipitation) to that typical of the 2003 flood (caused by 556 mm of precipitation) would decrease peak discharge at Tongguan by 8880 m^3/s (14,560 m^3/s of 1977 and 5680 m^3/s of 2003), shorten flood duration by 10 h (90 h in 1977, and 80 h in 2003) as well as the duration of the rising limb of flood by 8 h (48 h in 1977 and 40 h in 2003), and decrease peak water level by 0.7 m (327.5 m a,s,l in 1977 and 326.8 m a.s.l. in 2003). In both cases backwater would trace to Chenchun (Fig. 9). In turn, with channel roughness and river bed slope of 1977, the same reduction in flood wave volume would decrease peak discharge at Tongguan by 8620^3/s (14,230 m^3/s in 1977 and 5610 m^3/s in 2003), shorten flood duration by 17 h (107 h in 1977, and 90 h in 2003) as well as the duration of the rising limb of the flood by 10 h (55 h in 1977 and 45 h in 2003) and decrease peak water level by 0.2 m (328.5 m a.s.l. in 1977 and 328.3 m a.s.l. in 2003). Again, in both cases backwater would trace back to Chenchun. Finally, with channel roughness and river bed slope of 2003, the same reduction in flood wave volume would decrease peak

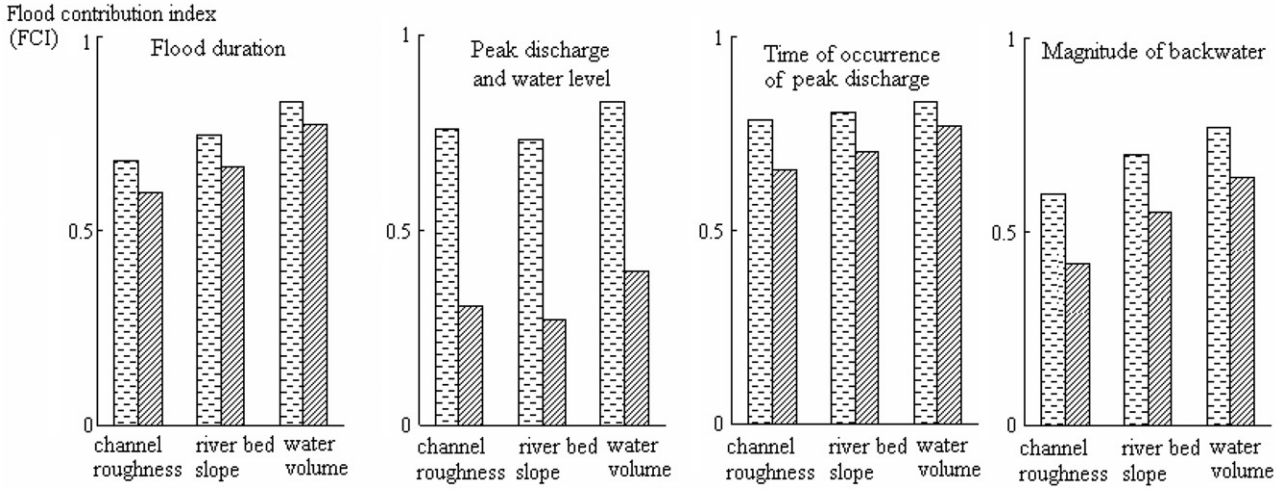

Figure 10 Integrated analysis of flood routing under combined scenarios in the middle Yellow River (the vertical axis of the graphs is flood contribution index which designs to evaluate the contribution to flood wave propagation of river bed slope, channel roughness, and water volume amount in flood routing).

discharge at Tongguan by 6390 m^3/s (11,590 m^3/s in 1977 and 5200^3/s in 2003), shorten flood duration by 18 h (237 h in 1977, and 219 h in 2003), as well as the duration of the rising limb of the flood by 10 h (55 h in 1977 and 45 h in 2003), and decrease peak water level by 1.7 m (331.0 m a.s.l. in 1977 and 329.4 m a.s.l. in 2003). With both flood wave volumes, backwater would trace back to Chenchun.

Fig. 10 shows the effects of model parameters, such as river bed slope, channel roughness, and flood wave volume on flood routing. Flood wave volume has the greatest impact on flood duration, peak discharge and water level, the time of occurrence of peak discharge, and magnitude of backwater, whereas, channel roughness has the second strongest impact on flood duration and magnitude of backwater. Conditionally, channel roughness also has the second strongest impact on peak discharge and water level. Of the model parameters, flow discharge has the strongest influence on flood wave propagation and backwater effects. At high flood discharges, bed slope has the stronger effect on flood routing than channel roughness, whereas at relatively low flood discharges, roughness is more important.

Conclusions

The study examined the methodology of combining hydrodynamic computational schemes with river basin characteristics of multiple tributaries in the middle Yellow River basin in China. Unlike many others, the proposed schemes link environmental and geomorphologic characteristics to flood wave propagation with a downstream backwater effect of complex flood routing. Clearly, calibration and validation with historical flood events improve our understanding of backwater characteristics in bidirectional flow as well as convergent and divergent flows between the main channel and tributaries. Moreover, the hydrodynamic computational schemes developed in the study are able to increase numerical stability required in computing complex flood routing processes, since the stability of the numerical scheme is strongly associated with the adaptation of channel descritization in computation. The study demonstrated that using dedicated computation schemes according to different types of floods can improve our understanding of the mechanism of flood flow propagation. By examining the simple scheme, improved scheme and the scheme for bidirectional flow, the results provided several important insights into the complex flood routing processes related to the occurrence of backwater effect. It was identified that some characteristics of the inflow hydrograph are sensitive to modelling accuracy, such as the geometric form of the hydrograph and its peak flow. In general, the study concludes with following summaries:

First, the boundary conditions can significantly alter flood routing processes. The backwater resulting from divergent flows and bidirectional flood flows can delay the occurrence and extend the duration of peak flow. This conclusion is supported by the simulation results for convergent and divergent flood flows in the middle of Yellow River basin for the years 1962—2003. Especially, the shape of hydrographs changed from tall and thin to low and wide. The evidence for the delayed occurrence and extended duration of peak flows after the 1960s and for the intensification of the trends after the early 1980s is important for the management of the Yellow River and its tributaries.

Second, the study identified variables influencing the flood routing process. The analysis of combined boundary conditions showed that water volume has the greatest impacts on flood duration, peak discharge and water level, the time of occurrence of peak discharge, and the magnitude of backwater. River bed slope has the second strongest impacts on flood duration and the magnitude of backwater. In turn, channel roughness has the second strongest impacts on peak discharge and water level. However, the influence that river bed slope and channel roughness exert on flood routing will depend on internal boundary conditions and the amount of backwater in the study reach.

Finally, the model successfully described that abrupt fluctuation of boundary conditions increases the magnitude of backwater. The simulation indicated that the backwater occurs under the conditions of convergent and divergent flows, as well as bidirectional flows. For the convergent and divergent flows, backwater is usually generated when flow discharges in the main river are greater than those in the tributaries. For the bidirectional flows, backwater is caused by convergence of two flood waves of similar magnitudes from the opposite directions. The evidence of intensified backwater events after the 1980s confirmed that human activities, such as the construction of the Sanmenxia Dam, exerted significant influence on flood characteristics in the middle Yellow River basin due to the flood routing boundary conditions. Due to the population increases world wide, the impacts of human activity on hydrological system need to be understood in order to prevent unexpected consequences. The hydrodynamic computational schemes proposed in this article should represent a significance value internationally.

Acknowledgements

The study was partially supported by a grant of the Chinese Academy of Sciences (KZCX3-SW-146), and a grant of USA Office of Navy Research (Grant No.: N00014-06-10220). Authors sincerely appreciate the constructive comments and editorial suggestions from two anonymous reviewers.

References

Begin, Z.B., 1986. Curvature ratio and rate of river bend migration update. Journal of Hydraulic Engineering 112 (10), 904—908.

Beven, K.J., Wood, E.F., Sivapalan, M., 1988. On hydrological heterogeneity — catchment morphology and catchment response. Journal of Hydrology 100 (1—3), 353—375.

Camacho, L.A., Lees, M.J., 1999. Multilinear discrete lag-cascade model for channel routing. Journal of Hydrology 226 (1—2), 30—47.

Carrivick, J.L., 2006. Application of 2D hydrodynamic modelling to high-magnitude outburst floods: an example from Kverkfjoll, Iceland. Journal of Hydrology 321 (1—4), 187—199.

Carson, M.A., Griffiths, G.A., 1989. Gravel transport in the braided Waimakariri River: mechanisms, measurements and predictions. Journal of Hydrology 109 (3—4), 201—220.

Chung, W.H., Aldama, A.A., Smith, J.A., 1993. On the effects of downstream boundary conditions on diffusive flood routing. Advance of Water Resource 19, 259—275.

Cunnane, C., 1988. Methods and merits of regional flood frequency analysis. Journal of Hydrology 100, 269–290.

Daluz, V.J.H., 1983. Conditions governing the use of approximations for the Saint-Venant equations for shallow surface water flow. Journal of Hydrology 60, 43–58.

Goel, N.K., Kurothe, R.S., Mathur, B.S., Vogel, R.M., 2000. A derived flood frequency distribution for correlated rainfall intensity and duration. Journal of Hydrology 288, 56–67.

He, H., Zhou, J., Yu, Q., Tian, Y.Q., Chen, R.F., 2006. Flood frequency and routing processes at a confluence of the middle Yellow River in China. River Research and Applications 22, 1–21.

Keskin, M.E., Agiralioglu, N.A., 1997. Simplified dynamic model for flood routing in rectangular channels. Journal of Hydrology 202, 302–314.

Lee, K.T., Chang, C.H., 2005. Incorporating subsurface-flow mechanism into geomorphology-based IUH modelling. Journal of Hydrology 311 (1–4), 91–105.

Marston, R.A., Girel, J., Pautou, G., Piegay, H., Bravard, J.P., Arneson, C., 1995. Channel metamorphosis, floodplain disturbance, and vegetation development: Ain River, France. Geomorphology 13, 121–131.

Mosselman, E., 1995. A review of mathematical models of river plan form changes. Earth Surface Processes and Landforms 20, 661–670.

Nash, J.E., Sutcliffe, J.V., 1970. River flow forecasting through conceptual models, 677 Part 1 — a discussion of principles. Journal of Hydrology 10 (3), 282–290.

Qian, L., 1992. Climate of the Loess Plateau, China. Meteorological Press, Beijing, pp. 213–256.

Ramamurthy, A.S., 1990. Dividing flow in open channels. Journal of Hydraulic Engineering 116 (3), 449–455.

Ren, X., Cheng, J., 2003. River Hydrology. Hohai University Press, Nanjing, pp. 110–143.

Schuurmans, J., Bosgra, O.H., Brouwer, R., 1995. Open-channel flow model approximation for controller design. Applied Mathematical Modelling 19 (9), 525–530.

Speight, J.G., 1965. Flow and channel characteristics of the Angabunga River, Papua. Journal of Hydrology 3 (1), 16–36.

State Flood Control and Drought Relief Headquarters, 1992. Flood Control Handbook. China Science Press, Beijing, pp. 230–256.

Thorne, S.D., Furbish, D.J., 1995. Influences of coarse bank roughness on flow within a sharply curved river bend. Geomorphology 12, 241–257.

Tsai, C.W., 2005. Flood routing in mild-slope rivers-wave characteristics and downstream backwater effect. Journal of Hydrology 308, 151–167.

USGS. <http://wwwrcamnl.wr.usgs.gov/sws/fieldmethods/Indirects/nvalues/index.htm>.

Walters, R.A., Cheng, R.T., 1980. Accuracy of an estuarine hydrodynamic model using smooth elements. Water Resources Research 16, 187–195.

Wang, X., 2004. The research on the flood peak flow forecast of Jiaokou in flood season. Journal of Northwest Hydroelectric 20 (3), 62–64.

Wang, X., Du, J., Wu, M., 2005. Situation analysis of rain, water and disaster for catastrophic flood in lower reaches of Weihe River in August, 2003. Journal of Natural Disasters 14 (3), 44–50.

Webb, R.H., Leake, S.A., 2006. Ground-water surface-water interactions and long-term change in riverine riparian vegetation in the southwestern United States. Journal of Hydrology 320 (3–4), 302–323.

Wharton, G., Arnell, N.W., Gregory, K.J., Gurnell, A.M., 1989. River discharge estimated from channel dimensions. Journal of Hydrology 106 (3–4), 365–376.

Wyzga, B., 1997. Methods for studying the response of flood flows to channel change. Journal of Hydrology 198, 271–288.

Yu, S., Lin, X., 1996. Abrupt change of drought/flood for the last 522 years in the middle reaches of yellow. Quarterly Journal of Applied Meteorology 7 (1), 89–95.